Polym. Korea, Vol. 49, No. 4, pp. 512-517 (2025)
https://doi.org/10.7317/pk.2025.49.4.512
ISSN 2234-8077(Online)

내성 *Helicobacter Pylori* 제균 치료를 위한 Levofloxacin 정전기 복합체 제조 및 평가

이준학[#] · 박성모[#] · 김재열 · 이창수 · 김상우 · 조관형[†]
인제대학교 약학대학
(2025년 4월 2일 접수, 2025년 4월 29일 수정, 2025년 4월 29일 채택)

Preparation and Characterization of Levofloxacin Electrolyte Complex for Eradication of Resistant *Helicobacter Pylori*

Jun Hak Lee[#], Sung Mo Park[#], Jae Yeol Kim, Chang Soo Lee, Sang Woo Kim, and Kwan Hyung Cho[†]
College of Pharmacy and Inje Institute of Pharmaceutical Sciences and Research, Inje University, Gimhae 50834, Korea
(Received April 2, 2025; Revised April 29, 2025; Accepted April 29, 2025)

초록: 본 연구의 목적은 내성 *Helicobacter pylori*(HP)를 제거하기 위해 양이온성 퀴놀론계 항생제인 레보플록사신(LFX)과 음이온성 고분자인 람다 카라기난(LCN)을 사용하여 정전기 복합체(EC)를 제조하고 물리화학적 특성을 평가하여 최적화하는 것이었다. EC는 LFX와 LCN의 농도 비율 및 용액 pH를 변화시키며 초음파 진동을 가하여 제조하였고, 입자 크기와 봉입률을 분석하였다. 그 결과, EC는 미립자이면서 봉입률이 90% 이상으로 높게 나타났다. 선정된 EC(F3)는 DSC, XRD, FTIR 및 SEM을 사용한 특성 평가에서 LFX와 LCN이 정전기 결합에 의해 무정형의 10 μm 보다 작은 미립자를 형성하고 있음을 확인하였다. 용출시험에서는 F3의 용출률이 2 시간까지 pH 1.2 >> pH 4.0 > pH 6.8의 순서를 나타내며 위 지향성 약물 방출을 보였다. 따라서 이 연구에서 제조된 F3는 내성 HP 감염 치료를 위한 새로운 약물 전달 시스템으로 활용될 가능성을 확인하였다.

Abstract: This study developed an electrolyte complex (EC) by combining levofloxacin (LFX), a cationic quinolone antibiotic, with λ-carrageenan (LCN), an anionic polymer, to target resistant *Helicobacter pylori* infections. Various EC formulations were prepared using ultrasonication, adjusting the concentration ratios of LFX and LCN and the solution pH. Particle size and encapsulation efficiency were the primary parameters evaluated. The results indicated that the ECs formed microparticles with encapsulation efficiencies exceeding 90%. The optimized formulation, F3, was characterized using DSC, PXRD, FTIR, and SEM, which revealed that electrostatic interactions between LFX and LCN produced an amorphous complex with particle sizes below 10 μm. *In vitro* dissolution tests demonstrated that F3 released the drug most rapidly at pH 1.2, followed by pH 4.0 and pH 6.8, confirming its potential for stomach-targeted drug delivery. As a result, the F3 identified in this study may be used as a new drug delivery system to treat resistant HP infections.

Keywords: *Helicobacter pylori*, levofloxacin, λ-carrageenan, electrolyte complex, stomach-targeted drug delivery system.

Introduction

Helicobacter pylori (HP) is a spiral-shaped Gram-negative bacterium that infects the gastric mucosa, producing a variety of gastrointestinal diseases such as gastritis, peptic ulcers, and gastric cancer.[1] Approximately 50% of the global adult population is infected with HP, with the global prevalence of HP infection estimated to be 43.1% between 2011 and 2022.[2,3] The standard three-drug therapy for HP eradication includes a proton pump inhibitor (PPI) and two antibiotics (amoxicillin, clarithromycin, or metronidazole).[4] However, rising antibiotic resistance has reduced the efficacy of conventional HP eradication therapy.[5] The World Health Organization (WHO) reports a global average resistance rate of 32.6% for clarithromycin and 35.3% for metronidazole.[6] Overcoming the limitations of conventional antibiotic therapies requires the development of successful alternative strategies.[7,8]

Levofloxacin (LFX) is a fluoroquinolone antibiotic that inhibits DNA gyrase, interfering with DNA replication. It has

[#]These authors equally contributed to this work.
[†]To whom correspondence should be addressed.
Chokh@inje.ac.kr, ORCID 0000-0003-1667-7625

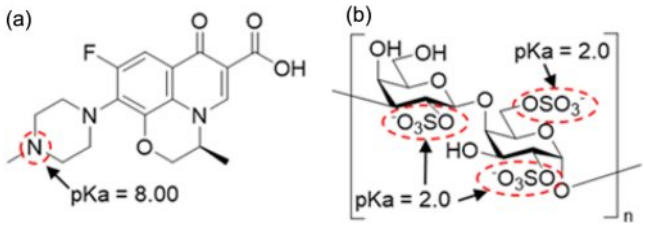

Figure 1. Chemical structure of (a) LFX; (b) LCN.

excellent tissue penetration, a long half-life, and powerful antibacterial activity.[9,10] LFX is more effective against resistant strains of conventional antibiotics and combining antibiotics with diverse modes of action has a synergistic inhibitory effect on HP resistance.[11] Global treatment guidelines advocate the combination of LFX and amoxicillin as a second or third-line treatment for resistant HP and is widely used as a key therapeutic strategy for controlling antibiotic resistance. Figure 1(a) depicts the chemical structure of levofloxacin, which is designated as (S)-9-fluoro-2,3-dihydro-3-methyl-10-(4-methylpiperazin-1-yl)-7-oxo-7H-pyrido[1,2,3-de]-1,4-benzoxazine-6-carboxylic acid, with the piperazinyl group in its structure having a pKa value of 8. Therefore, below neutral pH, binding with hydrogen ions results in a positive charge.

λ-carrageenan (LCN) is a hydrophilic anionic polymer derived from seaweed, commonly used as a thickening agent, gelling agent, and stabilizer.[12,13] It has a high potential for usage in drug delivery systems. Figure 1(b) shows that the sulfate functional groups present in the structure of LCN have a low pKa value, resulting in a negative charge when in solution. As a result, electrostatic interactions with diverse cationic drugs have the potential to produce an electrolyte complex (EC).[14-16]

ECs are prepared by electrostatic interactions in which positively and negatively charged substances spontaneously bind together, they can be used in a variety of drug delivery systems based on the physicochemical properties of the drug and polymer.[17] Such complexes improve the solubility and stability of the drug. Furthermore, the manufacturing process is straightforward, and the complex can be prepared by simple mixing of drug solution and polymer solution, eliminating the need for additional excipients, and making it cost-effective. Under certain conditions, the drug and polymer interact naturally, resulting in higher encapsulation efficiency and drug stability.[18-20] In addition, LCN exhibits mucoadhesive properties, allowing EC to adhere to the mucus layer where HP resides, thereby enhancing localized drug delivery and therapeutic efficacy.[21]

In this study, ECs were prepared by allowing LFX and LCN to react in a pH-adjusted solution through simple mixing. The particle morphology, size, encapsulation efficiency, and physical state were studied, and dissolution testing was conducted to assess stomach-targeted drug dissolution.

Experimental

Materials. Levofloxacin anhydrous (LFX, >98.0%) was purchased from Aladdin Industrial Corporation (Shanghai, China), and λ-carrageenan (LCN, viscosity >10 mPa·s with 0.3% carrageenan in H_2O at 25 ℃) was obtained from TCI Chemical Industry Co., LTD (Tokyo, Japan). All other solvents and reagents were used as received, with no additional purification.

Preparation of EC. LFX (500 mg) was placed in a beaker containing 45 mL of acetate buffer (50 mM, pH 4.0) and stirred until completely dissolved. The pH of this solution was adjusted to the corresponding pH of F1-F6 as specified in Table 1, by adding 1N HCl or 1 N NaOH dropwise while stirring. The solution was then transferred into a 50 mL volumetric flask. An acetate buffer was added to the final volume. This was the LFX solution. The amount of LCN for each formulation, as given in Table 1 (F1 = 250 mg, F2 = 500 mg, F3-F6 = 1500 mg), was added to a beaker containing 45 mL of acetate buffer (50 mM, pH 4.0) and stirred until it was completely dissolved. The pH of this solution was adjusted to the corresponding pH of F1-F6 as specified in Table 1, by adding 1 N HCl or 1 N NaOH dropwise while stirring. The solution was then transferred to a 50 mL volumetric flask, and acetate buffer was added to the final volume. This was the LCN solution. The ECs for each formulation (Table 1) were prepared in a beaker by mixing the LCN and LFX solutions using an ultrasonic homogenizer (VCX 500; Sonics & Materials Inc., Newtown, CT, USA). After cooling to room temperature, the pH of the final EC suspension was determined using a pH meter (SevenCompact S220; Mettler Toledo, Columbus, OH, USA).

Particle Size Analysis of EC. The particle size of the prepared ECs was determined using a nanoparticle size analyzer (NanoBook 90Plus; Brookhaven Instruments Corporation, Nashua, NH, USA) after diluting it 10 times with 50 mM ace-

Table 1. Composition of EC Formulation (F1-F6)

		F1	F2	F3	F4	F5	F6
LFX solution	LFX (w/v %)	1.0	1.0	1.0	1.0	1.0	1.0
	Solution pH	4.0	4.0	4.0	2.0	3.0	5.0
LCN solution	LCN (w/v%)	0.5	1.0	3.0	3.0	3.0	3.0
	Solution pH	4.0	4.0	4.0	2.0	3.0	5.0

tate buffer at the same pH. The mean and standard deviation of each sample were computed after three independent measurements.

Encapsulation Efficiency (%) of LFX in EC. EC solution (3 mL) was taken by pipette and centrifuged at 15000 rpm for 15 min at room temperature using a centrifuge (LZ-1730R; LaboGene, Seoul, Republic of Korea). The supernatant (1 mL) was obtained and diluted 400 times with 50 mM acetate buffer (sample solution). LFX standard (10 mg) was dissolved with 200 mL of 50 mM acetate buffer (pH 4.0), and this solution was diluted 4 times with 50 mM acetate buffer (standard solution). The absorbance of the produced samples and standard solutions was determined at 293 nm using a UV-Vis spectrophotometer (UV-1800; SHIMADZU Corp., Kyoto, Japan). We used the following equation to compute the LFX encapsulation efficiency (%) based on the obtained absorbance:

$$\text{Encapsulation efficiency (\%)} = \left(1 - \frac{A_{\text{sample}}}{A_{\text{standard}}}\right) \times 100 \quad (1)$$

where A_{sample} represents the absorbance of the sample solution at 293 nm, and A_{standard} refers to the absorbance of the standard solution at 293 nm. The encapsulation efficiency was measured three times, and the mean and standard deviation were calculated.

Differential Scanning Calorimetry (DSC). The thermal behaviors of the LFX, LCN, and F3 samples and the physical mixture corresponding to the F3 samples were examined using DSC (DSC Q20; TA Instruments, New Castle, DE, USA). The prepared solution was filtered through a 0.45 μm membrane filter to obtain F3 samples and dried in open air at room temperature (20-25 ℃) for at least 24 h. These samples were also analyzed using the following powder X-ray diffraction (PXRD), Fourier transform infrared spectroscopy (FTIR), and scanning electron microscope (SEM) techniques. Each sample (3-5 mg) was placed in an aluminum pan, and the thermal response was examined while increasing the temperature from 30 ℃ to 350 ℃ at a heating rate of 10 ℃/min.

Powder X-Ray Diffraction (PXRD). An X-ray diffractometer (Ultima IV, Rigaku Corp., Tokyo, Japan) with a LinXeye 1-D detector was used to conduct PXRD analysis on the LFX, LCN, and F3 samples and the physical mixture. The X-ray source was set to 40 kV and 40 mA to produce Cu-Kα radiation. To prevent preferred orientation, each 20 mg sample was attached to a grid, and the diffraction pattern was recorded over a range of 7° to 40° at a scanning rate of 2°/min.

Fourier Transform Infrared Spectroscopy (FTIR). A 5 mg sample of LFX, LCN, F3, and the physical mixture were placed in the sample holder. The spectra were recorded across a range of 4000 cm^{-1} to 600 cm^{-1} using an FTIR spectrometer (Varian 640-IR, Varian Medical Systems, Inc., Palo Alto, CA, USA) fitted with an attenuated total reflection (ATR) accessory.

Scanning Electron Microscope (SEM) Analysis. Morphological studies of LFX, LCN, and F3 were analyzed using field-emission scanning electron microscopy (FE-SEM; S-4300, Hitachi, Tokyo, Japan). Each sample (3-5 mg) was fixed onto a carbon tape and coated with a 15 nm thick platinum layer, after which the particles were observed at an acceleration voltage of 15 kV and a working distance of 5 mm.

***In vitro* Dissolution Study.** The dissolution test was performed using USP Dissolution Apparatus II at a rotation speed of 50 rpm and a temperature of 37.0 ± 0.5 ℃ using a VK 7000 dissolution tester (VanKel Technology Group, Cary, NC, USA). The dissolution media were HCl/NaCl buffer (pH 1.2), 45 mM acetate buffer (pH 4.0), and 50 mM phosphate buffer (pH 6.8), each with a volume of 900 mL.[22] A pipette was used to add 10 mL of the prepared F3 solution (containing equivalent LFX 50 mg) directly to each vessel. This dilution effect by the sample volume was considered when calculating the drug release %. Samples were collected in 5 mL aliquots at predetermined time intervals. The samples were filtered through a 0.45 μm PTFE filter and tested for LFX content using a UV-Vis spectrophotometer with an absorbance of 293 nm. The test was performed in triplicate, and the mean and standard deviation were calculated.

Results and Discussion

Particle Size and Encapsulation Efficiency of EC. The concentration ratios of LFX to LCN were evaluated under three different conditions (1:0.5, 1:1, and 1:3) with the results shown in Figure 2. The encapsulation efficiency of LFX in F1-F3 tended to increase as the concentration ratio of LCN increased, reaching 38.67 ± 2.2%, 71.01 ± 2.1%, and 90.78 ± 2.3%, respectively. F3 had microparticles with a very small particle size (2935.3 ± 200.0 nm). F4-F6, with pH 2.0, pH 3.0, and pH 5.0, respectively, showed high encapsulation efficiency (F4 = 86.78 ± 2.12%, F5 = 90.08 ± 2.23%, and F6 = 90.81 ± 2.33%) and small particle size (F4 = 1957.70 ± 223.42 nm, F5 = 2949.40 ± 305.92 nm, and F6 = 2033.10 ± 288.11 nm). According to these findings, the optimum reaction concentration ratio between LFX and LCN for encapsulation efficiency was at 1:3. At pH 2-pH 5, LFX and LCN formed EC spontaneously due to electrostatic

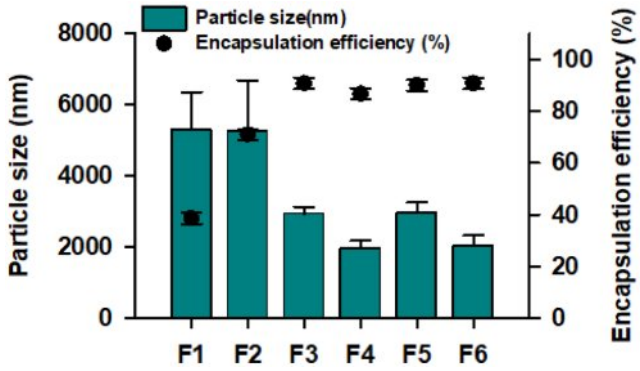

Figure 2. Particle size and encapsulation efficiency (%) of EC formulation.

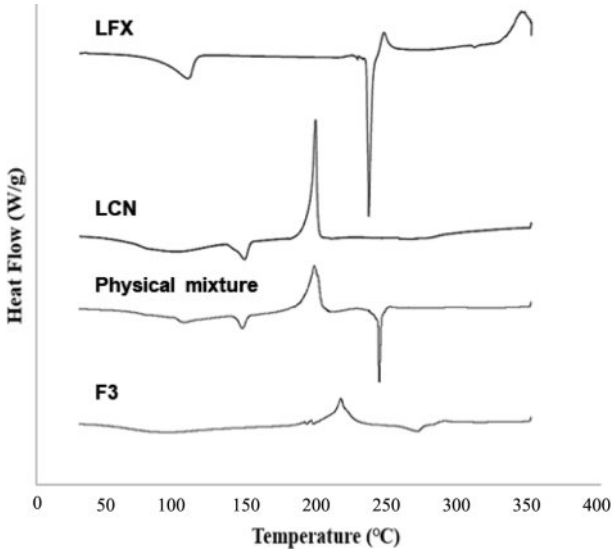

Figure 3. DSC curve of LFX, LCN, physical mixture, and F3.

interactions. Sonication may be effective in reducing particle size and enhancing the uniformity. Structurally, the sulfate functional groups of LCN have a strong negative charge, whereas the piperazine functional groups of LFX have a strong positive charge, resulting in an insoluble EC suspension.

DSC. Figure 3 shows the DSC curves for LFX, LCN, physical mixture, and F3. LFX shows endothermic peaks at 110 ℃ and 235 ℃, indicating crystal water desorption and intrinsic melting point, respectively. LCN has an endothermic peak at approximately 150 ℃. The physical mixture exhibited endothermic peaks from LFX and LCN at 110 ℃, 235 ℃, and 150 ℃. However, in F3, the LFX and LCN peaks disappeared, and there was no distinct endothermic peak indicating the LFX crystallinity loss during EC formation.

PXRD. Figure 4 shows the PXRD patterns for LFX, LCN, the physical mixture, and F3. LFX had a crystalline form with

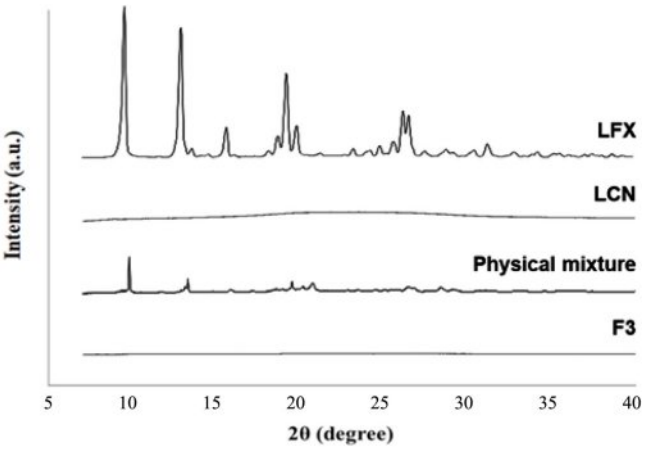

Figure 4. PXRD pattern of LFX, LCN, physical mixture, and F3.

distinct peaks at 9.5°, 12.9°, 19.2°, and 26.2°, whereas LCN was amorphous with no crystalline peaks. The intrinsic crystalline peaks of LFX were weakened owing to dilution with LCN in the physical mixture. F3 showed no crystalline peaks for LFX, indicating that LFX lost its crystallinity and became amorphous during EC preparation. The DSC and PXRD data showed that the interaction between LFX and LCN was driven by electrostatic interactions rather than recrystallization or precipitation, and that LFX was amorphous in EC.

FTIR. Figure 5 shows the FTIR spectra for LFX, LCN, and F3. F3 showed weaker peaks at 600 cm^{-1} to 2000 cm^{-1} and 2802 cm^{-1} compared with those of LFX and LCN. In the physical mixture, all the peaks corresponding to LFX and LCN remained unchanged. The sulfate functional group of LCN was

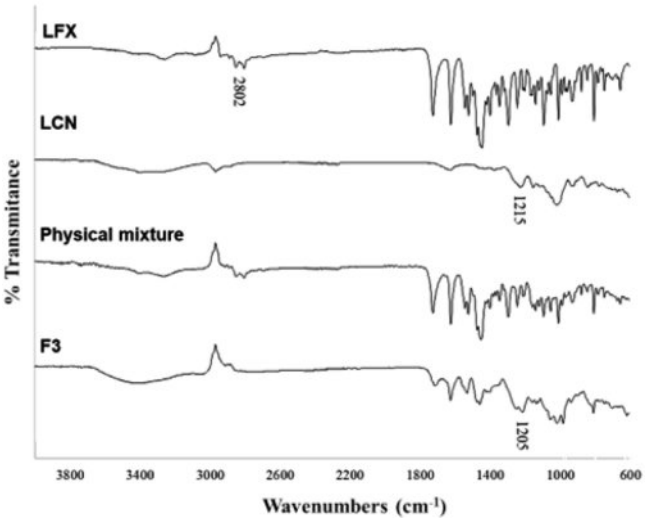

Figure 5. FTIR spectra of LFX, LCN, physical mixture, and F3.

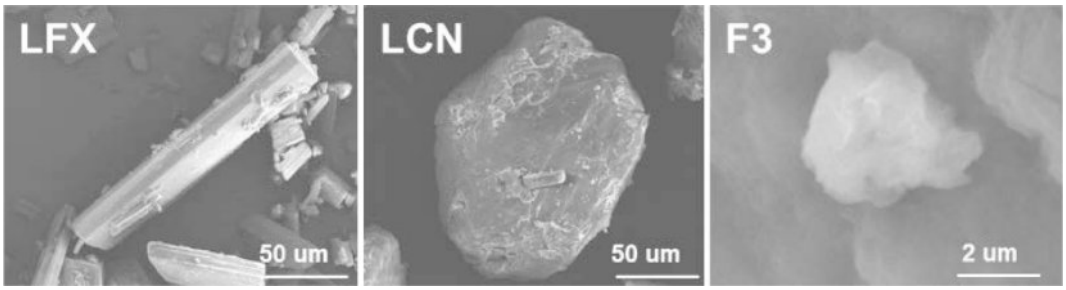

Figure 6. SEM image of LFX, LCN, and F3.

divided into two peaks at 1205 cm^{-1} in F3 due to interactions with the LFX, whereas the LFX only showed a single peak at that wavenumber.[23] The spectrum change in F3 indicates electrostatic interactions between the sulfate group of LCN and the piperazinyl group of LFX.

SEM Analysis. Figure 6 depicts the SEM images of LFX, LCN, and F3. LFX exhibited a rod-shaped crystalline habit with a length of >50 μm, while LCN was seen as a spherical particle with a size of >100 μm. F3 had a particle size of less than 10μm, which was consistent with the previously reported particle size in Figure 2. This finding demonstrates that the intrinsic morphology of the original materials was lost during EC formation, and the F3 was in the particle size range of approximately 4-6 μm with distinct morphology.

In vitro Dissolution Study. Figure 7 shows the dissolution profile of F3. F3 had the highest LFX dissolution rate at pH 1.2, reaching 84.69 ± 2.27% in 5 min. The LFX dissolution rates at pH 6.8 and pH 4.0 were 69.07 ± 2.41% and 61.70 ± 2.80%, respectively, which were approximately 10% lower than those at pH 1.2. According to Maezawa et al., commercial LFX products have been shown to achieve complete LFX dissolution at pH 1.2 within 30 to 60 min.[24] However, the LFX dissolution from F3 was completed within 5 min, which was faster than the commercial products. The enhanced dissolution rate of F3 under acidic conditions would be attributed to the amorphous state of LFX and its small particle size (<10 μm), in comparison with the large crystalline particles in commercial tablets. Furthermore, the dissolution rates were in the order of pH 1.2 >> pH 4.0 > pH 6.8. These findings demonstrate that F3 exhibits stomach-targeted dissolution characteristics, attaining over 80% drug dissolution at both pH 1.2 and pH 4.0 at 120 min, highlighting its potential as an HP eradication therapy.

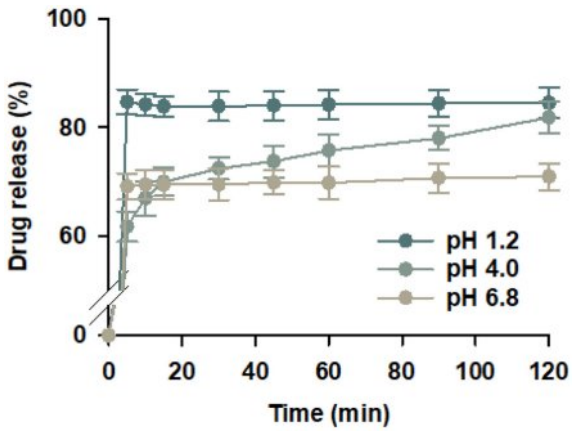

Figure 7. Dissolution curves of F3 in pH 1.2, pH 4.0, and pH 6.8.

Conclusions

In this study, an EC composed of the cationic quinolone antibiotic LFX and the anionic polymer LCN was developed for HP eradication therapy. The ECs were prepared using a simple mixing method. The optimized formulation, F3, had an LFX:LCN weight ratio of 1:3 (w/w) in a buffer (pH 4.0) and was an amorphous form. Furthermore, it demonstrated stomach-targeted dissolution properties, with over 80% drug dissolution within 5 min at pH 1.2 and pH 4.0. As a result, F3 is expected to be a promising formulation for HP eradication due to its high local antibiotic action in the gastric environment.

Acknowledgments: This work was supported by the 2023 Inje University research grant.

Conflict of Interest: The authors declare that there is no conflict of interest.

References

1. Malfertheiner, P.; Camargo, M. C.; El-Omar, E.; Liou, J. M.; Peek, R.; Schulz, C.; Smith, S. I.; Suerbaum. S. Helicobacter

Pylori Infection. *Nat Rev Dis Primers* **2023**, 19.
2. Hooi, J. K. Y.; Lai, W. Y.; Suen, M. M. Y.; Underwood, F. E.; Tanyingoh, D.; Malfertheiner, P.; Graham, D. Y.; Wong, V. W. S.; Wu, J. C. Y.; Chan, F. K. L.; Sung, J. J. Y.; Kaplan, G. G.; Ng, S. C. Global Prevalence of Helicobacter pylori Infection: Systematic Review and Meta-Analysis. *Gastroenterology* **2017**, 153, 420-429.
3. Li, Y.; Choi, H.; Leung, K.; Jiang, F.; Grajam, D. Y.; Leung, W. K. Global Prevalence of Helicobacter Pylori Infection Between 1980 and 2022: A Systematic Review and Meta-analysis. *Lancet Gastroenterology & Hepatology* **2023**, 8, 553-564.
4. Kate, V.; Kalayarasan, R; Ananthakrishnan, N. Sequential Therapy Versus Standard Triple-Drug Therapy for Helicobacter pylori Eradication: a Systematic Review of Recent Evidence. *Drugs* **2013**, 73, 815-824.
5. Fallone, C. A.; Moss, S. F.; Malfertheiner, P. Reconciliation of Recent Helicobacter pylori Treatment Guidelines in a Time of Increasing Resistance to Antibiotics. *Gastroenterology* **2019**, 157, 44-53.
6. Salahi-Niri, A.; Nabavi-Rad, A. N.; Monahan, T. M.; Rokkas, T.; Doulberis, M.; Sadeghi, A.; Zali, M. R.; Yamaoka, Y.; Tacconelli, E.; Yadegar, A. Global Prevalence of Helicobacter Pylori Antibiotic Resistance Among Children in the World Health Organization Regions Between 2000 and 2023: A Systematic Review and Meta-analysis. *BMC Medicine* **2024**, 598.
7. Gisbert, J. P.; Pajares, J. M. Helicobacter Pylori "rescue" Therapy After Failure of Two Eradication Treatments. *Helicobacter* **2005**, 10, 363-372.
8. Gisbert, J. P.; Morena, F. Systematic Review and Meta-analysis: Levofloxacin-based Rescue Regimens After Helicobacter Pylori Treatment Failure. *Aliment Pharmacol Ther.* **2006**, 23, 35-44.
9. Hurst, M.; Lamb, H. M.; Scott, L. J.; Figgitt, D. P. Levofloxacin. *Drugs* **2002**, 62, 2127-2167.
10. North, D. S.; Fish, D. N.; Redington, J. J. Levofloxacin, A Second-generation Fluoroquinolone. *Pharmacotherapy* **1998**, 18, 915-35.
11. Oliphant, C. M.; Green, G. M. Quinolones: A Comprehensive Review. *Am Fam Physician* **2002**, 65, 455-64.
12. Necas, J.; Bartosikova, L. Carrageenan: A Review. *Vet Med-Czech* **2013**, 58, 187-205.
13. Li, L.; Ni, R.; Shao, Y.; Mao, S. Carrageenan and Its Applications in Drug Delivery. *Carbohydrate Polymers* **2014**, 103, 1-11.
14. Antonov, Y. A.; Zhuravleva, I. L. Complexation of Lysozyme With Lambda Carrageenan: Complex Characterization and Protein Stability. *Food Hydrocolloids* **2019**, 87, 519-529.
15. Tapia, C.; Escobar, Z.; Costa, E.; Sapag-Hagar, J.; Valenzuela, F.; Basualto, C.; Gai, M. N.; Yazdani-Pedram, M. Comparative Studies on Polyelectrolyte Complexes and Mixtures of Chitosan–alginate and Chitosan–carrageenan as Prolonged Diltiazem Clorhydrate Release Systems. *Europ. J. Pharm. Biopharmaceutics* **2004**, 57, 65-75.
16. Heinen, C.; Reuss, S.; Saaler-Reinhardt, S.; Langguth, P. Mechanistic Basis for Unexpected Bioavailability Enhancement of Polyelectrolyte Complexes Incorporating BCS class III Drugs and Carrageenans. *Europ. J. Pharm. Biopharmaceutics* **2013**, 85, 26-33.
17. Mocchiutti, P.; Schnell, C. N.; Rossi, G. D.; Peresin, M. A.; Zanuttini, M. A.; Galván, M. V. Cationic and Anionic Polyelectrolyte Complexes of Xylan and Chitosan. Interaction with Lignocellulosic Surfaces. *Carbohydrate Polymers* **2016**, 150, 89-98.
18. Kindermann, C.; Matthée, K.; Sievert, F.; Breitreutz, J. Electrolyte-Stimulated Biphasic Dissolution Profile and Stability Enhancement for Tablets Containing Drug-Polyelectrolyte Complexes. *Pharm. Res.* **2012**, 29, 2710-2721.
19. Lankalapalli, S.; Kolapalli, V. R. Polyelectrolyte Complexes: A Review of their Applicability in Drug Delivery Technology. *Indian J. Pharm. Sci.* **2009**, 71, 481-487.
20. Mónica, C. G.; Julio C. C.; Clarisa I. R.; Paulina L. P.; Miriam C. S.; Ruben H. M.; Fabiana L. A.; Cecilia I. A. I.; Alvaro F. J. K. A Novel Gel Based on An Ionic Complex From a Dendronized Polymer and Ciprofloxacin: Evaluation of Its Use for Controlled Topical Drug Release. *Mater. Sci. Eng. C* **2016**, 69, 236-246.
21. Yermak, I. M..; Davydova, V. N.; Kravchenko, A. O.; Chistyulin, D. A.; Pimenova, E. A.; Glazunov, V. P. Mucoadhesive Properties of Sulphated Polysaccharides Carrageenans from Red Seaweed Families Gigartinaceae and Tichocarpaceae. *Int. J. Biolog. Macromol.* **2020**, 142, 634-642.
22. Park, J. W.; Lee, S.-W.; Lee, J. H.; Park, S. M.; Cho, S. J.; Maeng, H.-J.; Cho, K. H. Supersaturated Gel Formulation (SGF) of Atorvastatin at a Maximum Dose of 80 mg with Enhanced Solubility, Dissolution, and Physical Stability. *Gels* **2024**, 10, 837.
23. Nasrazadani, S.; Eghtesad, R.; Sudoi, E.; Vupputuri, S.; Ramsey, J. D.; Ley, M. T. Application of Fourier Transform Infrared Spectroscopy to Study Concrete Degradation Induced by Biogenic Sulfuric Acid. *Mater Struct* **2016**, 49, 2025-2034.
24. Maezawa, K.; Yajima, R.; Terajima, T.; Kizu, J.; Hori, S. Dissolution Profile of 24 Levofloxacin (100 mg) Tablets. *J. Infection Chemotherapy* **2013**, 19, 996-998.